TGS 203 - Carbon Monoxide Sensor Specifications

1. Structure and Dimensions

Please refer to the technical drawing shown in Figure 1. Specifications for component parts subject to Table I below.

2. Materials

Part numbers are as indicated in the technical drawing of Figure 1.

#	Part	Material
1	Stainless Steel Gauze	Stainless Steel SUS 304 (60 mesh)
2	Activated Charcoal Filter	20 ~ 40-mesh
3	Cover	Polyamide resin reinforced with glass fiber
4	Sensor Element	Metal oxide semiconductor
5	Flame-Proof Cover	Double layer of 100-mesh stainless steel gauze SUS 316
6	Coil	Paladium-Iridium alloy wire Diameter: 0.09mm
7	Base	Polyethylene terephthalate reinforced with glass fiber
8	Ring	Nickel plated brass ring
9	Pin	Nickel
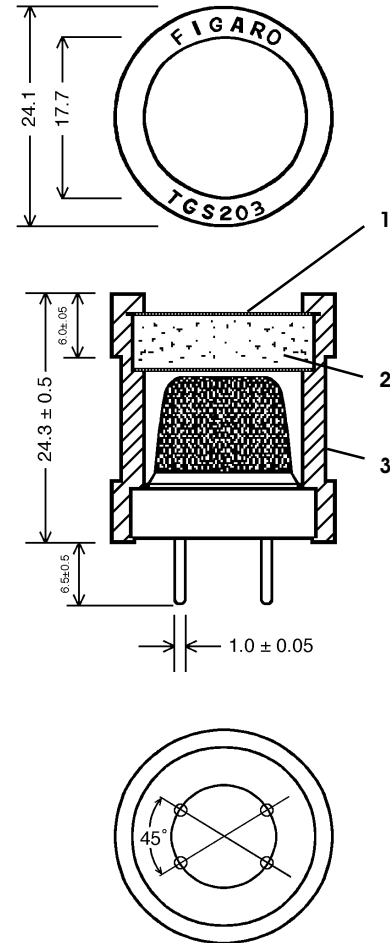
3. Explosion Proof

A spark inside the cover cannot ignite a gas leak outside of the cover.
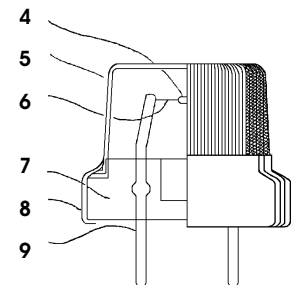
4. Mechanical Strength

Connecting Strength

Using applied pressure, a ring is affixed to the base for the purpose of holding the flame proof cover in a fixed position.

Withdrawal Force

The pins can withstand a withdrawal force of more than 5 kgs applied in the direction of the pins.


Cross section of internal sensing element

Figure 1

5. <u>Sensitivity Characteristics</u>

Item	Symbol	Condition	Specification
Sensor Resistance	Rs	CO at 100ppm	1kΩ ~ 15kΩ
Change Ratio of Sensor Resistance	Rs/Ro	$\dfrac{\text{Rs (H}_2\text{ at 1000ppm)}}{\text{Rs (CO at 100ppm)}}$	> 1.0
Sensor Resistance Gradient	α	$\dfrac{\log \text{(Rs in 100ppm CO/Rs in 300ppm CO)}}{\log \text{(100ppm CO/300ppm CO)}}$	-1.50 ~ -0.73

6. <u>Standard Test Conditions</u>

The TGS-203 complies with the above listed electrical characteristics when the sensor is tested using the circuit illustrated at the right and under the standard conditions set forth in the table below. V_{RL} shall be measured during the final 0.5 seconds of the low heater voltage period. The sensing unit shall be evaluated in the basic measuring circuit under the reference atmosphere immediately after a minimum of 96 hours of pre-heating.
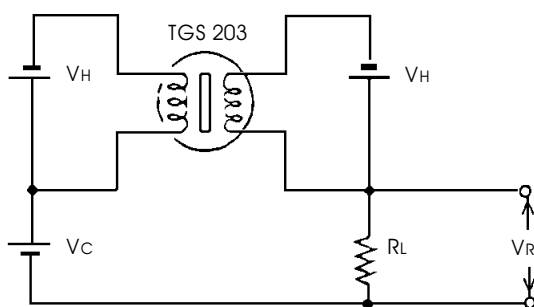
Basic Measuring Circuit

V_C - Circuit voltage R_L - Load resistance
V_{RL} - Output voltage V_H - Heater voltage

<u>NOTE</u>: Test gas must have greater than 99.9% purity under ambient conditions of 20˚C and 1 atm.

Item	Symbol	Rated Value	Remarks
Circuit Voltage	Vc	5.0V ± 1%	DC
Heater	V_H	V_{HH} = 0.8V ± 3% for 60 ± 1 sec. V_{HL} = 0.25V ± 3% for 90 ± 1 sec.	Must appliy alternately for duration specified
	I_H	I_{HH} = 369mA ± 3% for 60 ± 1 sec. I_{HL} = 133mA ± 3% for 90 ± 1 sec.	
Load Resistance	R_L	4KΩ ± 1%	
Reference Atmosphere		20˚C ± 2˚C, 65% ± 5% RH	Test chamber must have > 1 liter capacity

Sensor Resistance (Rs) is calculated by the following formula:

$$R_S = \frac{V_C - V_{RL}}{V_{RL}} \times R_L$$

Power dissipation across sensor electrodes (Ps) is calculated by the following formula:

$$P_S = \frac{(V_C - V_{RL})^2}{R_S}$$

Technical Information for Carbon Monoxide Sensors

The marketing of TGS203 started in 1980 as a semiconductive type carbon monoxide sensor featuring high selectivity and stability. Since then, this sensor has been one of the best selling tin dioxide sensors produced by Figaro Engineering Inc.

See also Technical Brochure "Technical Information on Usage of TGS Gas Sensors for Explosive/Toxic Gas Alarming".

IMPORTANT NOTE: OPERATING CONDITIONS IN WHICH FIGARO SENSORS ARE USED WILL VARY WITH EACH CUSTOMER'S SPECIFIC APPLICATIONS. FIGARO STRONGLY RECOMMENDS CONSULTING OUR TECHNICAL STAFF BEFORE DEPLOYING FIGARO SENSORS IN YOUR APPLICATION AND, IN PARTICULAR, WHEN CUSTOMER'S TARGET GASES ARE NOT LISTED HEREIN. FIGARO CANNOT ASSUME ANY RESPONSIBILITY FOR ANY USE OF ITS SENSORS IN A PRODUCT OR APPLICATION FOR WHICH SENSOR HAS NOT BEEN SPECIFICALLY TESTED BY FIGARO.

---

1. Specifications

1-1 *Features*

* High sensitivity and selectivity to carbon monoxide (CO)
* Low sensitivity to alcohol and hydrogen
* Minimal effect by nitrogen oxide (NOx) coexisting with CO
* Long life

1-2 *Applications*

* Residential and commercial CO detectors
* Air quality controllers
* Ventilation control for indoor parking garages

1-3 *Structure*

Figure 1 shows the structure of TGS203. Tin dioxide (SnO_2) is used as the main material of the sensor element. A pair of wire electrodes are embedded in the sintered material. A 90-micron diameter iridium-palladium alloy wire with resistance of approximately 2Ω is spot welded to nickel pins. The sensor base is made of polyethylene terephthalate reinforced with glass fiber. The internal cover is a double layer of 100 mesh stainless steel gauze (SUS316) and the cover is fastened to the sensor base by a nickel-plated brass ring. The external housing material consists of reinforced polyamide resin (UL94V-0) and a layer of 60 mesh stainless steel gauze (SUS304) is used for the outside cover. The space layer between the internal cover and outer cover is filled with activated charcoal.
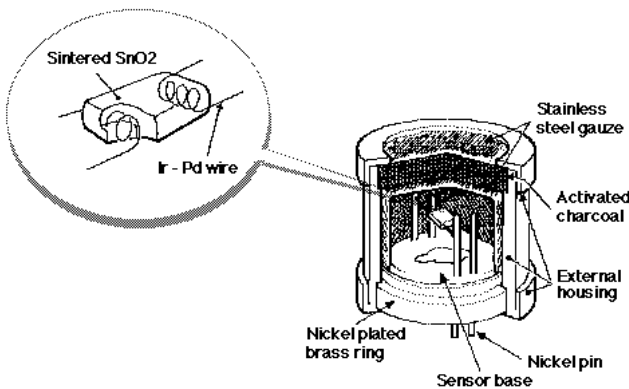
1-4 *Basic measuring circuit*

Figure 2 shows the basic measuring circuit of the TGS203. Circuit voltage (Vc) is applied across the sensor element which has a resistance (Rs) between the sensor's two electrodes and a load resistor (RL) connected in series. The temperature of the sensor element is controlled by heaters located at both sides of the sensor to which a high and low voltage cycle is applied according to the timetable shown in Figure 3. A 60 second high heater voltage period heat cleans the sensor, purging humidity (an interference gas) which may build up in the sensor's crystal structure during the low heater cycle. A 90 second low heater voltage cycle conditions the sensor element at the optimal temperature for sensing. Measurement for the presence of gas is performed only during a 0.5 second period at the conclusion of the low heater voltage period. The sensor signal (VRL) is measured as a change in voltage across the RL.
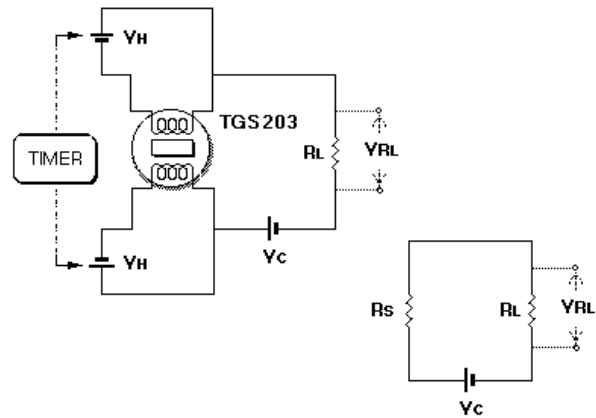
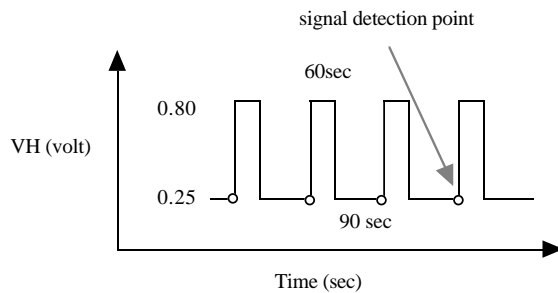Figure 2 - Basic measuring circuit
(including equivalent circuit)

Figure 1 - Sensor structure

Figure 3 - High/Low cycle of heater voltage

1-5 *Circuit & operating conditions*

The following conditions should be maintained to ensure stable sensor performance:

Item	Rating
Circuit Voltage (Vc)	5.0V ± 1% DC
Heater voltage (V$_H$)	V$_{HH}$ = 0.8V ± 3% for 60±1 sec. V$_{HL}$ = 0.25V ± 3% for 90±1 sec. *(apply alternately for specified period)*
Heater current (I$_H$)	I$_{HH}$ = 369mA±3% for 60±1 sec. I$_{HL}$ = 133mA±3% for 90±1 sec. *(apply alternately for specified period)*
Heater resistance (room temp.)	1.85Ω .
Load resistance (R$_L$)	variable
Power dissipation (P$_S$)	less than 15mW
Signal detection timing	within 0.5 sec. prior to application of V$_{HH}$
Operating & storage temp.	-40˚C ~ +70˚C
Optimal detection concentration	50ppm ~ 1000ppm

1-6 *Specifications* [NOTE 1]

Item	Specification
Sensor resistance (**Rs**-100ppm of CO)	1kΩ ~ 15kΩ
Sensor resistance gradient (α)	-1.50 ~ -0.73
$\alpha = \dfrac{\log\{Rs(100ppm\ of\ CO)/Rs(300ppm\ of\ CO)\}}{\log(100ppm/300ppm)}$	
Relative sensitivity to H$_2$ (γ)	> 1.0
$\gamma = \dfrac{Rs(1000ppm\ of\ H_2)}{Rs(100ppm\ of\ CO)}$	
Power consumption	approx. 0.59W at V$_{HH}$ approx. 0.07W at V$_{HL}$

NOTE 1: Sensitivity characteristics are obtained under the following standard test conditions:

(Standard test conditions)
Temperature and humidity: 20 ± 2˚C, 65 ± 5% RH
Circuit conditions: as specified in Section 5 and with
$\qquad RL = 4.0k\Omega \pm 1\%$
Preheating period: 7 days or more under standard circuit conditions

Formula for calculation of sensor resistance:

$$Rs = \frac{Vc \ x \ RL}{V_{RL}} - RL$$

Formula for calculation of sensor power dissipation:

$$Ps = Vc^2 Rs/(Rs + RL)^2$$

1-7 *Mechanical Strength*

The sensor shall have no abnormal findings in its structure and shall satisfy the above electrical specifications after the following performance tests:

<u>Withdrawal Force</u> - withstand force > 5kg in each direction

<u>Vibration</u> - frequency-1000c/min., total amplitude-4mm, duration-one hour, direction-vertical

<u>Shock</u> - acceleration-100G, repeated 5 times

1-8 *Dimensions*

top view

Unless otherwise specified, tolerance is ±0.5mm. Figures in parenthesis are for reference (u/m: mm)
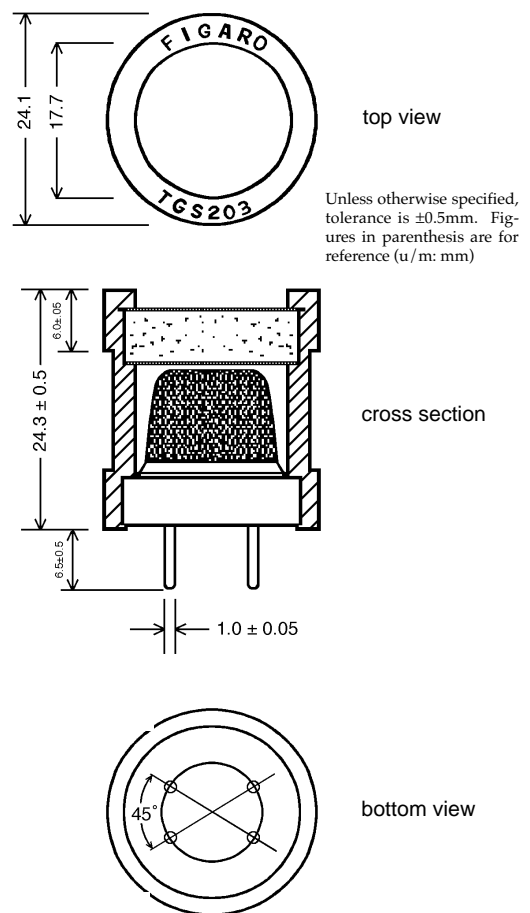
cross section

bottom view

Figure 4 - Dimensions

2. Operation Principle

Figure 5 shows the temperature of the sensor element surface (typical values) when the heater voltage (VH) varies. The temperature was measured through a thermocouple (CA, ø0.025mm) which was placed on the center of the sensor element's surface. The test was carried out in clean air at room temperature.

Note: Measurements were taken after application of heater voltage in order to stabilize sensor element surface temperature.
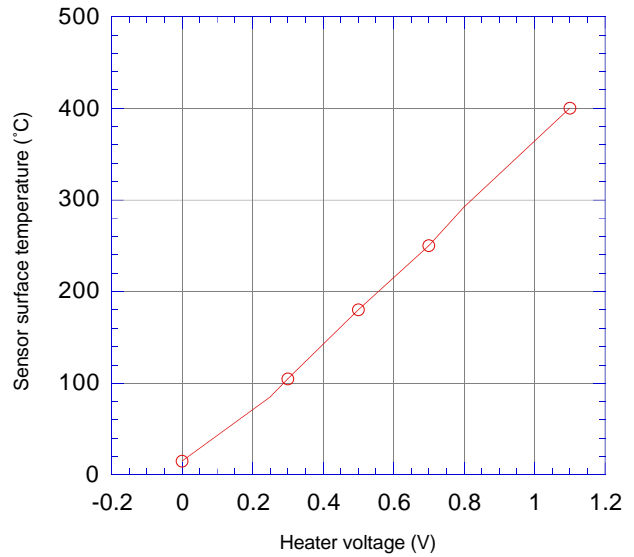
Figure 5 - Element surface temperature dependency on heater voltage

Figure 6 shows the manner in which sensitivity characteristics vary with changes to the sensor element temperature. Sensor resistance (Rs) in 2,000ppm of various gases was obtained by changing heater voltage (VH) as shown in Figure 5.

Figure 6 illustrates that the sensitivity to CO increases as the sensor element temperature is decreased and that the best selectivity to CO can be obtained if sensor element temperature is maintained under 100˚C. However, good reproducibility cannot be expected when the sensor is continuously used under 100˚C since the sensor becomes susceptible to the influence of water vapor or interference gases when this temperature is maintained for a prolonged period. To eliminate this influence, a cyclic high/low voltage as specified in *Section 1-5* is applied to the heater. High heater voltage heat-cleans the sensor by removing water vapor influence, while low heater voltage conditions the sensor for measuring CO gas.
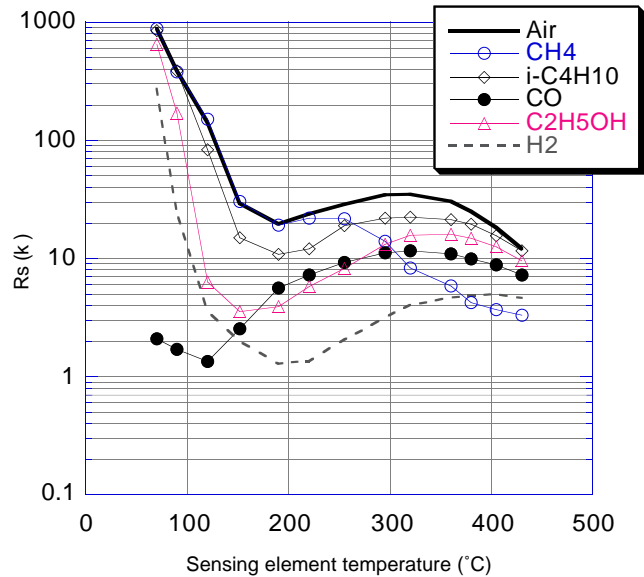
Figure 6 - Sensitivity dependency on element surface temperature

3. Basic Sensitivity Characteristics

3-1 *Sensitivity to various gases*

Figure 7 shows the sensor's relative sensitivity to various gases. The Y-axis shows the ratio of sensor resistance in various gases (Rs) to the sensor resistance in 100ppm of CO (Ro).

Sensor resistance in fresh air is several $M\Omega$ or more. The sensitivity to methane (CH_4) and propane (C_4H_{10}) is negligible. The sensitivity to hydrogen, hydrogen sulfide (H_2S), sulfur dioxide (SO_2), and ethanol (C_2H_5OH) is very low when compared to that of CO. While Rs decreases in CO gas, nitrogen dioxide (NO_2) causes sensor resistance to increase. However, the effect of as much as 50ppm of NO_2 is negligible—the dotted line in Figure 7 shows the sensitivity to CO when 50ppm of nitrogen dioxide coexists.

The slope of the sensitivity curve for CO flattens out when CO concentration reaches around 5,000ppm. This concentration would be the practical upper sensing limit of the sensor.

The amount of CO generated by cigarette smoke is roughly equivalent to 20ppm of CO when 10 cigarettes are smoked in a room of roughly 24 cubic meters in size. As a result, the influence of cigarette smoke itself would not be sufficient to cause the sensor to generate an alarm for residential detectors normally calibrated to alarm at 100ppm of CO.

3-2 *Temperature and humidity dependency*

Figure 8 shows the temperature and humidity dependency of TGS203. The Y-axis shows the ratio of sensor resistance in 100ppm of CO under various atmospheric conditions (Rs) to the sensor resistance in 100ppm of CO at 20°C and 65%RH (Ro).

An inexpensive way to compensate for temperature and humidity dependency to a certain extent would be to incorporate a thermistor in the detection circuit *(please refer to Section 5-3)*.
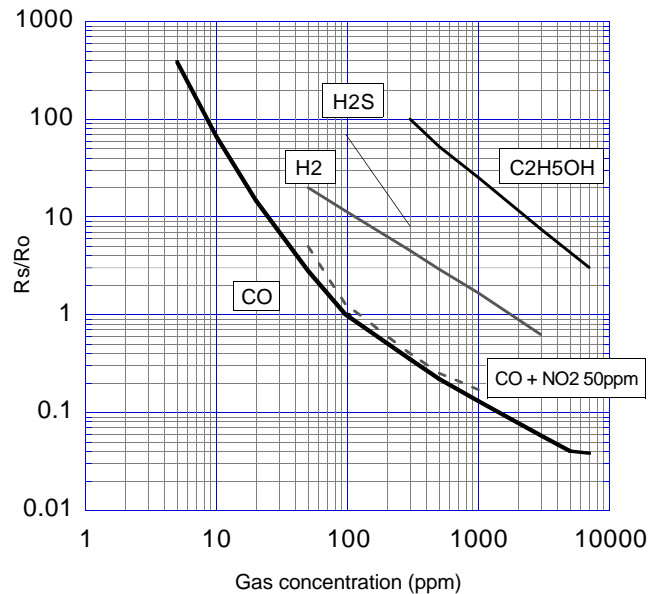

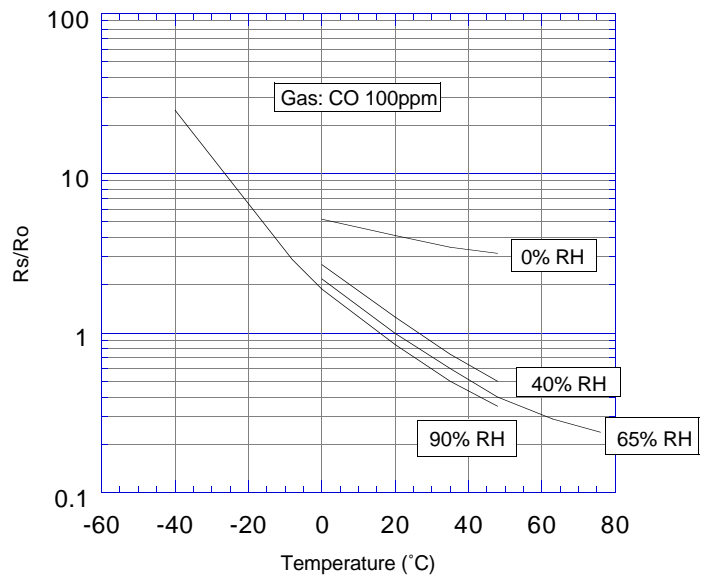Figure 7 - Sensitivity to various gases

Figure 8 - Temperature and humidity dependency

3-3 *Gas response pattern*

Figure 9-1 shows the change pattern of the sensor's output (V$_{RL}$) in 100ppm and 300ppm of CO respectively. Figure 9-2 shows the response of the sensor to 1000ppm of ethanol vapor.

These charts demonstrate the inverse relationship of V$_{RL}$ between CO and alcohol. In CO gas, the V$_{RL}$ starts increasing with the change in heater voltage to V$_{HL}$. After 90 seconds, when the heater voltage changes to V$_{HH}$, the V$_{RL}$ drastically increases for a short period of time and then decreases rapidly. Conversely, in ethanol vapor the V$_{RL}$ starts increasing with the change in heater voltage to V$_{HH}$ in a short time, and then the V$_{RL}$ starts decreasing. After 60 seconds, when the heater voltage changes to V$_{HL}$, the V$_{RL}$ rapidly decreases again in a short time and the V$_{RL}$ then reaches a stabilized value.

Figure 10 below shows the change in sensor element temperature which occurs during the sensor heating schedule. This chart explains the behavior of V$_{RL}$ in Figures 9-1 and 9-2. Sensitivity to CO is much greater at low temperatures and significantly reduced at high temperatures, while the inverse is true for ethanol sensitivity.
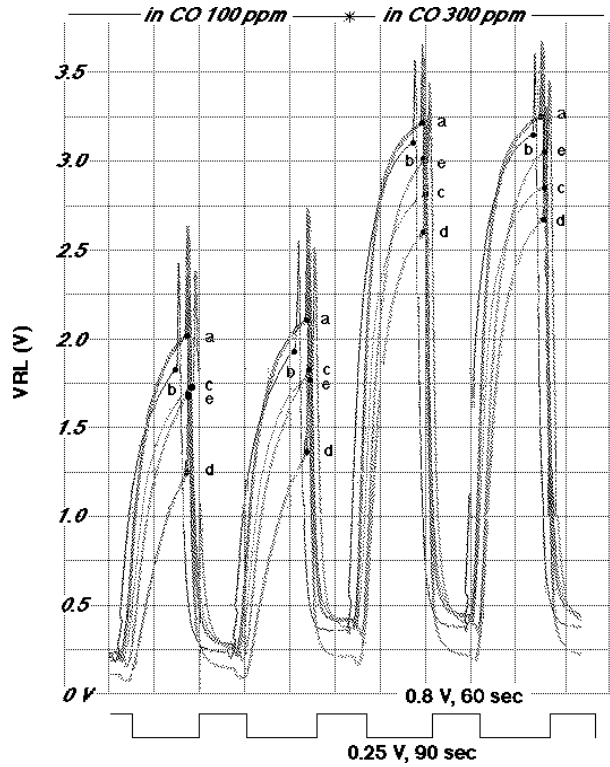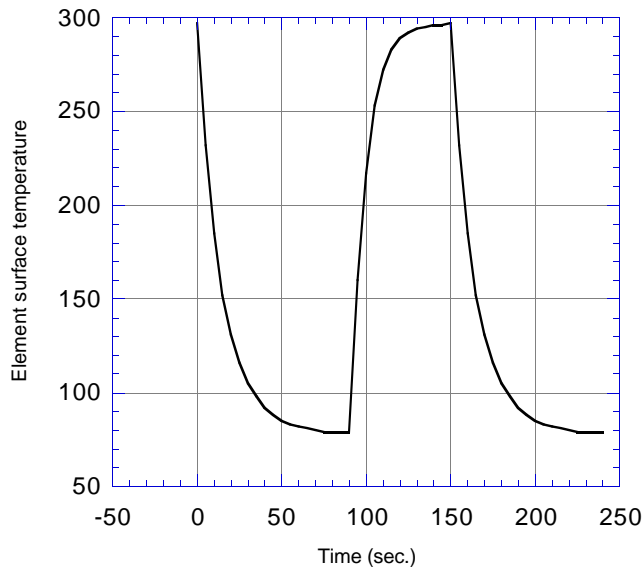

Figure 9-1 - CO response pattern

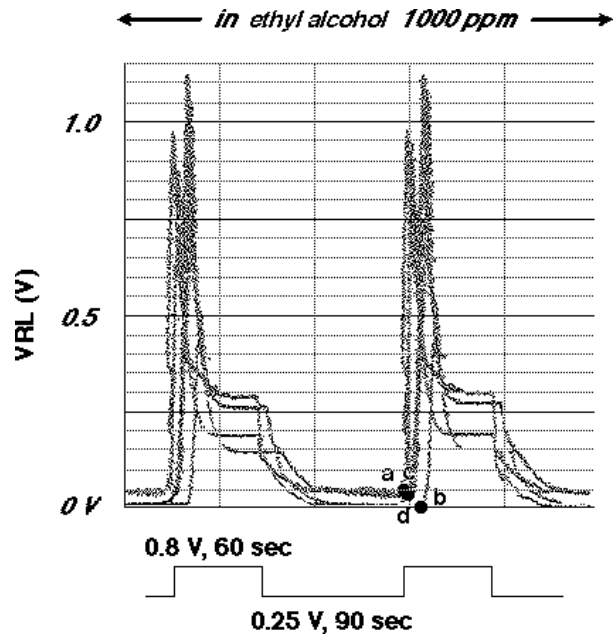
Figure 10 - Sensor element temperature change

Figure 9-2 - Ethanol vapor response pattern

3-4 *Heater voltage dependency*

Figure 11-1 shows the change in the sensor resistance ratio according to variation in V_{HL}. The Y-axis is the ratio of sensor resistance in various gases (Rs) versus Rs in 100ppm of CO when V_{HL}=0.25V (Ro). All measurements for purposes of this test were taken during the 0.5 second sensing period at the conclusion of the heating cycle (i.e. after V_{HL}).

When V_{HL} is higher than the rated value of 0.25V, the relative sensitivity of the sensor to hydrogen as compared to CO becomes higher. In contrast, when the V_{HL} is lower than the rated value of 0.25V, the relative sensitivity to H_2 compared to CO becomes smaller.
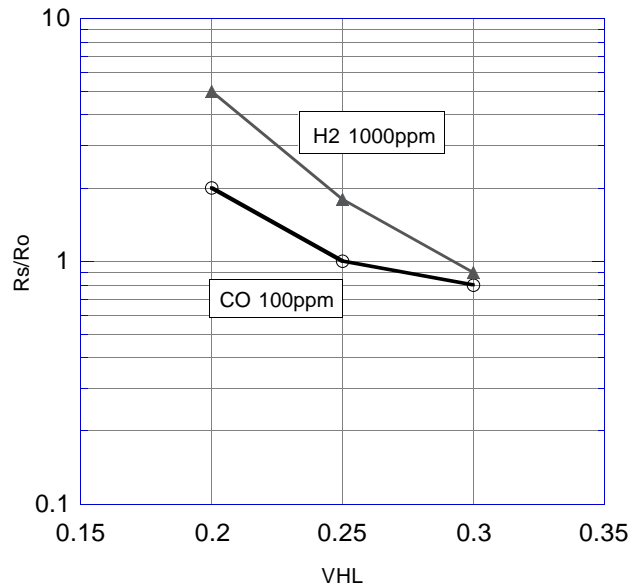
Figure 11-1 - Heater voltage dependency
(V_{HH} = 0.8V)

Figure 11-2 shows the variation in sensor resistance ratio according to variation in V_{HH}. The Y-axis is the ratio of sensor resistance in various gases (Rs) versus Rs in 100ppm of CO when V_{HH}=0.8V (Ro). Again all measurements for purposes of this test were taken during the 0.5 second sensing period at the conclusion of the heating cycle (i.e. after V_{HL}).

When V_{HH} is higher than the rated value of 0.8V, the relative sensitivity of the sensor to hydrogen as compared to CO becomes higher. In contrast, when the V_{HL} is lower than the rated value of 0.25V, the relative sensitivity to H_2 compared to CO becomes smaller. The sensitivity to ethanol is smallest at the rated value of V_{HH}.
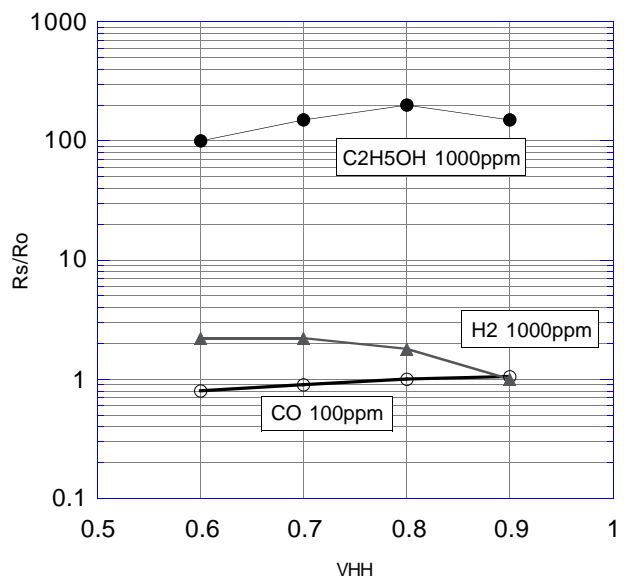
It should be noted that when V_{HL} or V_{HH} is lower than the rated value, short-term reproducibility becomes inferior, and CO sensitivity generally tends to decrease in the long term. When V_{HL} or V_{HH} is higher than the rated value, CO sensitivity generally tends to increase in the long term.

Figure 11-2 - Heater voltage dependency
(V_{HL} = 0.25V)

3-5 *Initial action*

Figure 12 shows the initial action of the sensor's voltage output (V_{RL}). For purposes of this test, the sensor was stored unenergized in normal air for 40 days after which it was energized in clean air.

After energizing, the V_{RL} at V_{HH} started off very high but gradually decreased to a stable level while the V_{RL} at V_{HL} was so low that an alarm delay circuit would not be required.
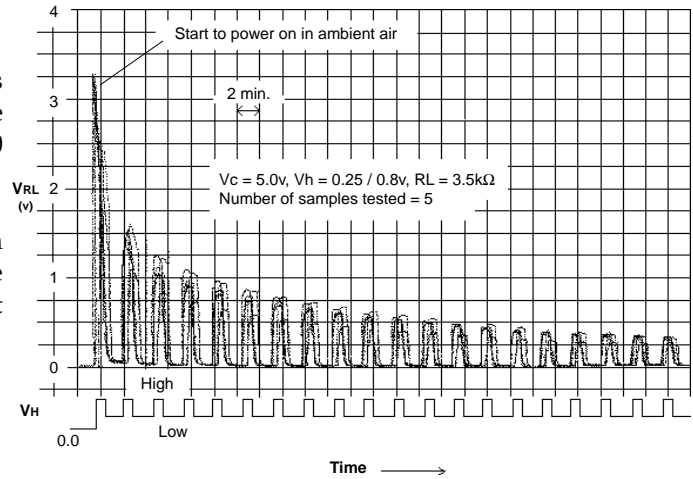
Figure 12 - Initial action

3-6 *Influence of unenergized storage*

Figure 13 shows the influence of unenergized storage on sensor resistance. Sensors were stored unenergized in normal air for 2 weeks, 4 weeks, and 3 months respectively after which they were energized. The Y-axis represents the ratio of sensor resistance in 100ppm of CO after various unenergized periods (Rs) to the resistance in 100ppm of CO after energizing at the rated voltage for 10 days (Ro).

These charts demonstrate that after energizing, sensor resistance first increases slightly and then returns to a stable level.
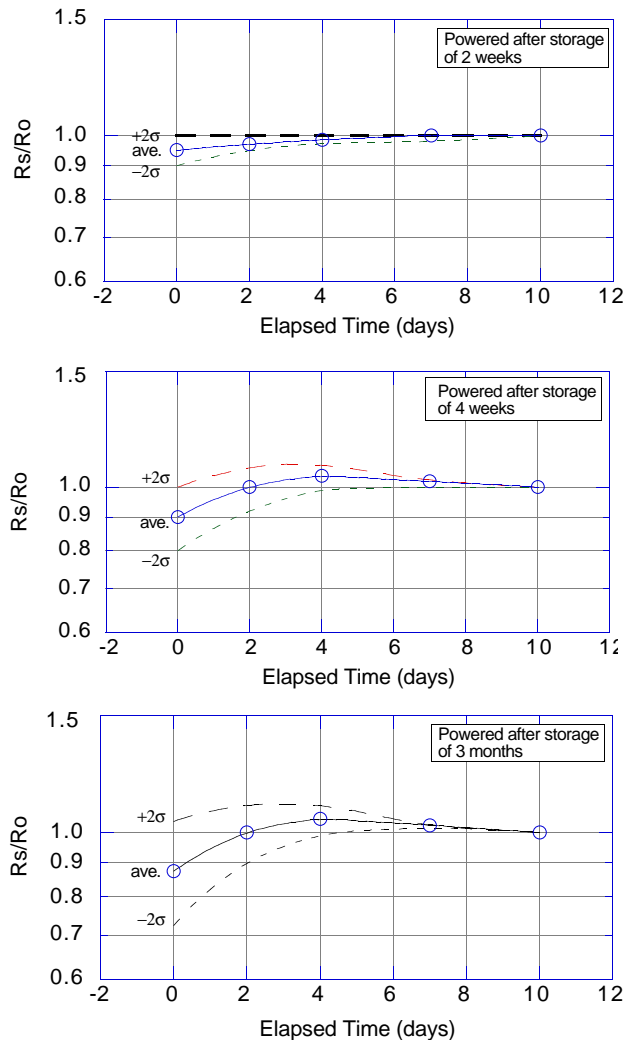
Figure 13 - Time dependency (Ro = 1.0)
(20 samples tested)

3-7 *Effect of the activated charcoal filter*

CO is commonly generated by the incomplete combustion of fossil fuels. For accurate detection of CO, it is necessary to eliminate the influence not only of alcohol in the atmosphere but also of NOx generated by such heating devices. To do so, TGS203 utilizes a filter of activated charcoal.

Figures 14-1 and 14-2 show sensitivity characteristics of TGS203 with and without the charcoal filter respectively.

As shown in Figure 14-1, sensitivity to alcohol is reduced by the filter and the influence of 50ppm of NO2 is virtually eliminated. The sensitivity to hydrogen is unaffected by the presence of the filter.

Note: Sensor resistance (Ro) in 100ppm of CO, which is used as a reference value in Figures 14-1 and 14-2, increases by approximately 50%~100% when measured with the filter.

Temperature and humidity dependency remains largely unaffected by the presence of the filter.
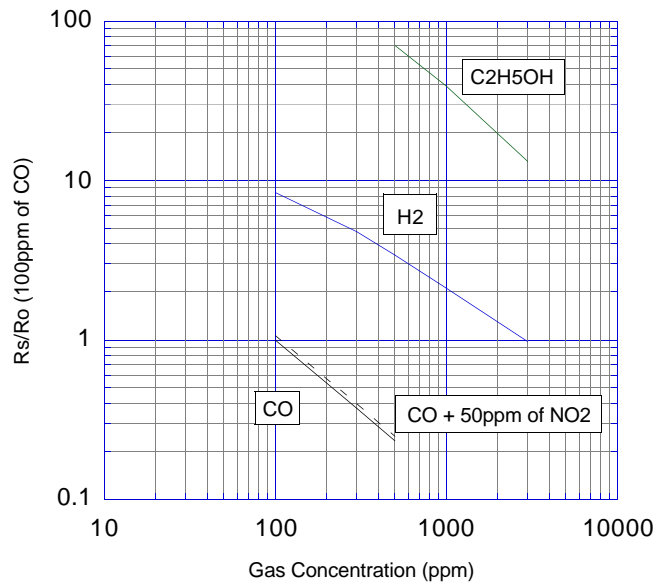
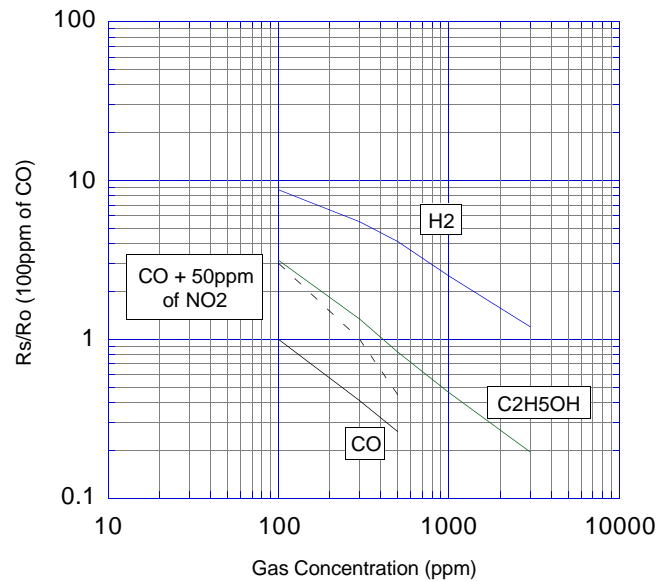Figure 14-1 - Gas sensitivity of TGS203
(with activated charcoal filter)

Figure 14-2 - Gas sensitivity of TGS203
(without activated charcoal filter)

4. Reliability

4-1 *Gas exposure test*

Figure 15 shows test conditions for short-term exposure of TGS203 to various gases. In this test, the sensor was kept energized under standard circuit conditions. Sensor resistance in 100ppm of CO was measured prior to the test gas exposure. After the exposure in gases according to the times shown in Figure 15, the sensor was removed from the test gas and energized in normal air. After one hour elapsed, sensor resistance in 100ppm of CO was again measured.
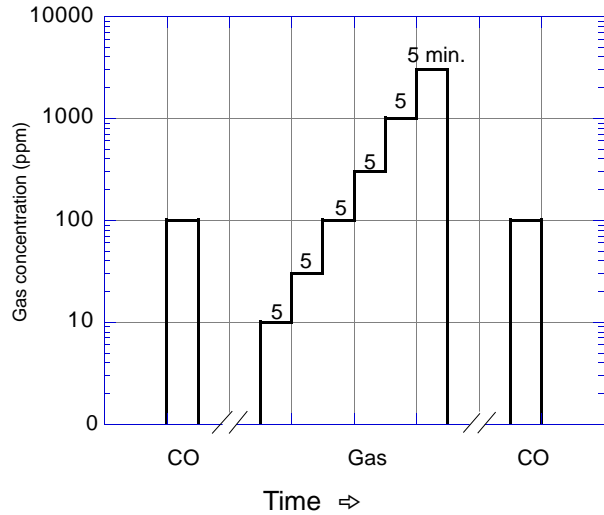
Exposure to 1000ppm and 3000ppm of test gas (last step in Figure 15) was not conducted for the following highly corrosive gases: hydrogen sulfide (H_2S), sulfur dioxide (SO_2), and nitrogen dioxide (NO_2).

Figure 16 shows the test results. The change ratio of sensor resistance in 100ppm of CO before and after exposure to the test gas is plotted. Most test gases caused some decrease in sensor resistance. Especially the influence of hydrogen sulfide and sulfur dioxide were remarkable. The sensor's ability to recover to original value from gas exposure is coded on Figure 16 as follows:

      1 - quick recovery
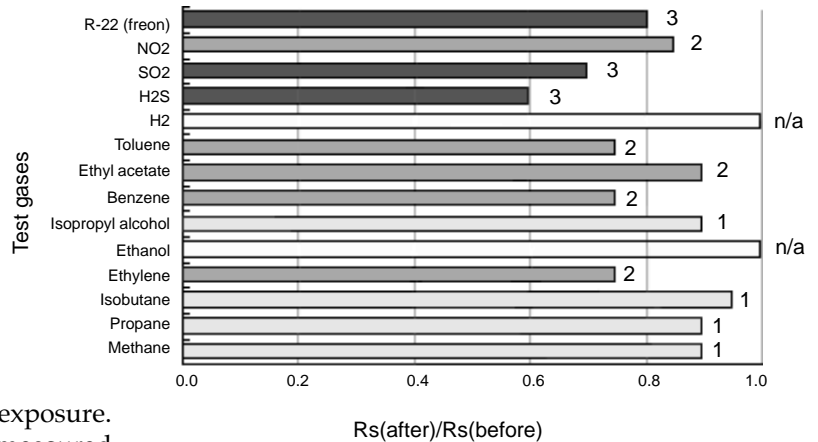   2 - recovery within one day
      3 - more than 7 days

Table 1 shows test results on long term gas exposure. Sensor resistance in 100ppm of CO was measured before long term gas exposure (Ro) after which the sensors were placed in an enclosed capacity vessel with a test gas for a designated period. The sensors were then removed and kept under normal environmental conditions for one hour prior to measuring their resistance in 100ppm of CO after exposure to test gas (Rs).

As these tests demonstrate, care should be taken to minimize exposure to gases which lower the sensor's sensitivity.

Figure 15 - Conditions of gas exposure test

Figure 16 - Effects of exposure to various gases

Table 1 - Long term exposure to various gases

Type of exposure (gas/conc./time)			Ambient condition	Sensor condition	Rs/Ro	# samples
SO_2	0.4ppm	10 days	50˚C/40%RH	energized	0.85	3
CH_4	2.5% for 7 hrs. + 20% H_2 for 1 hr.		room temp.	energized	0.70	5
H_2S	1000ppm	10 days	room temp.	energized	0.50	5
SO_2	5000ppm + 1% CO_2 for 10 days		room temp.	unenergized	0.15	5
4 cigarettes/13 liters			room temp.	energized	0.85	3
0.3cc salad oil/13 liters			room temp.	energized	0.85	3
CO	300ppm for 30 sec., pause 1 min., repeat 1000 times		room temp.	energized	0.98	3
Styrene	2000ppm	40 days	50˚C	unenergized	1.00	10
Toluene	2000ppm	40 days	50˚C	unenergized	1.00	10
Hexane	2000ppm	40 days	50˚C	unenergized	0.78	10
Acetone	2000ppm	40 days	50˚C	unenergized	0.98	10
Ethanol[1]	2000ppm	40 days	50˚C	unenergized	0.51	10
MEK[2]	2000ppm	40 days	50˚C	unenergized	0.81	7
1-1-1TCE[3]	2000ppm	40 days	50˚C	unenergized	0.87	10

[1] Sensor recovered Ro after energizing for 20 days in normal air
[2] Methyl ethyl ketone
[3] Trichloroethane

4-2 *Long-term stability*

Figure 17 shows long-term stability data for TGS203 for more than 8 years. Test samples were energized in normal air and under standard circuit conditions. Measurement for confirming sensor characteristics was conducted under standard test condition (20˚C, 65%RH). The initial value was measured after two days of energizing in normal air at the rated voltage.

The Y-axis shows the alarm concentration calculated by the sensor's resistance when the alarm concentration is set at 100ppm of CO. At the very beginning of energizing, alarm concentration increases, and then gradually decreases. After 8 years, the alarm concentration decreased to roughly one half of its initial value.
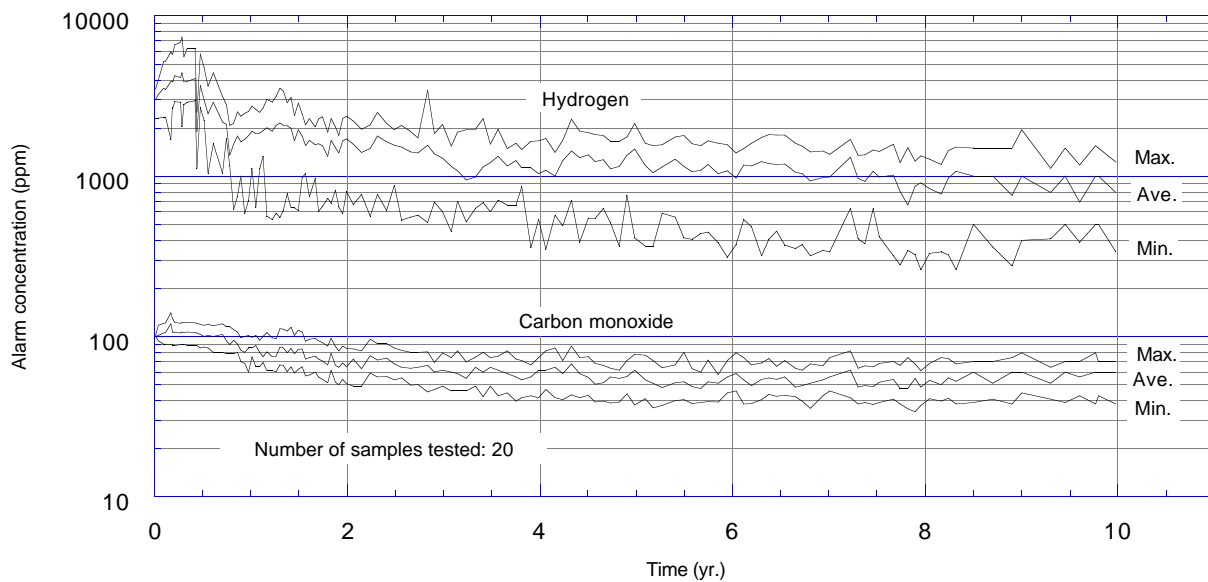

Figure 17 - Long term stability

4-3 *Durability of the activated charcoal filter*

(1) Effect of storage in normal air

In Figure 18, the effect of NO2 on a sensor stored for 3.5 years in normal air and a new sensor with a new filter are plotted. Virtually no difference in the ability of the sensor to eliminate the effects of NO2 can be seen between the two samples.
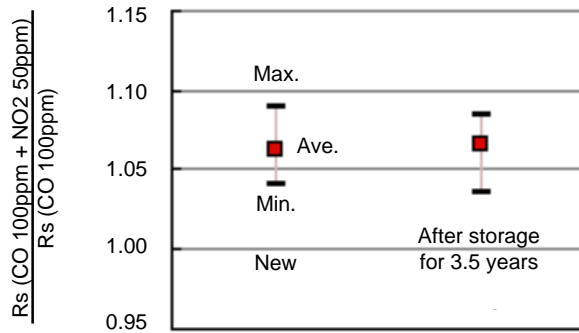
Figure 18 - Effect of being stored in normal air

(2) Effect of high temperature and high humidity

In Figure 19, the effect of NO2 is plotted for a sensor stored for two months under conditions of 50°C and 90%RH and for a new sensor with a new filter. This figure demonstrates that high temperature and humidity have almost no effect on the activated charcoal filter's ability to eliminate the effects of NO2.
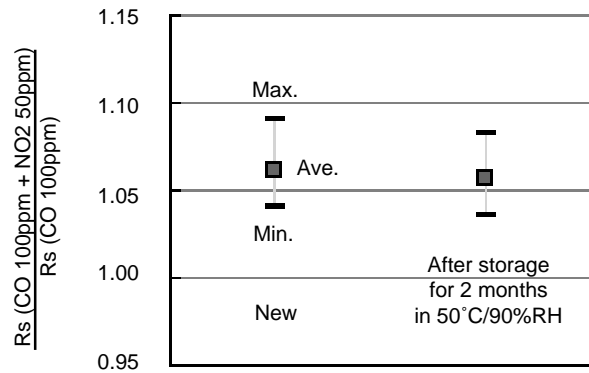
Figure 19 - Effect of high temperature/humidity

(3) Effect of long-term energizing

In Figure 20, the filter's performance in eliminating the effects of NO2 and alcohol vapor is compared for three different types of samples:

    * new filter
    * filter used on sensor energized for one year
    * filter used on a sensor energized for 7 years

These sample filters were placed on new sensor elements for conducting this test. The results show that as the energizing period becomes longer, performance in removing NO2 and alcohol vapor tends to decrease. However, the level of degradation in this performance is minimal and does not reach a level which would be a problem in practical usage.
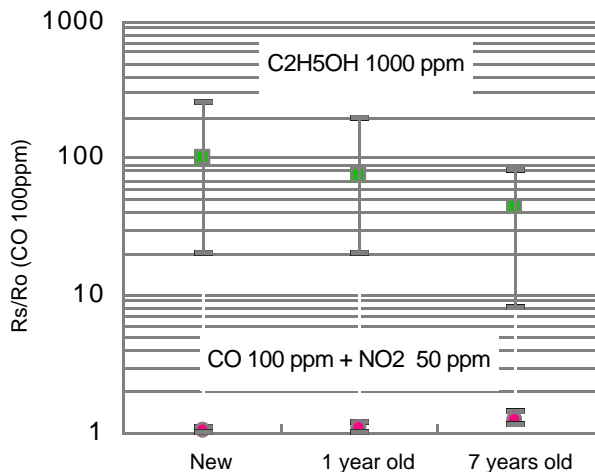
Figure 20 - Effect of long-term energizing

5 Circuit Examples

5-1 *Sensor signal measuring method*

Figures 21-1 and 21-2 show the sensor signal measuring method in circuits where a regulated current is applied to the heater in order to heat the sensor element. When heating the sensor element, Q1 and Q2 are closed as shown in Figure 21-1. When reading the sensor signal, Q1 and Q2 are opened as shown in Figure 21-2. The voltage applied to R_L is used as a sensor signal. The operation of Q1 and Q2 is controlled according to the conditions specified in *Section 1-5* by way of a time control IC such as a microcomputer.
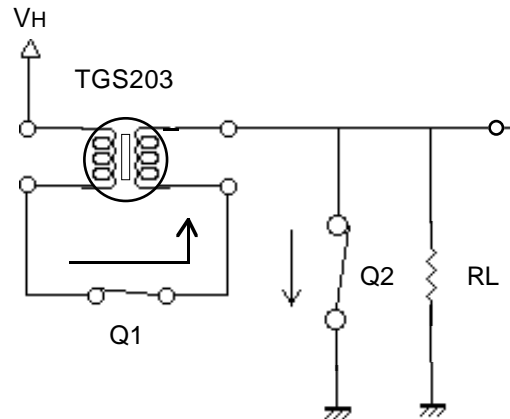

Figure 21-1 - Element heated period

5-2 *Sensor heater breakage detection circuit*

Sensor heater breakage can be detected by a resistor connected to Q2 in series. The voltage applied to the resistor is used as a monitor.
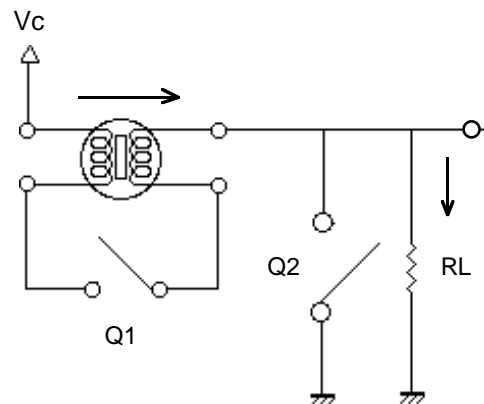
5-3 *Temperature compensation circuit*

The temperature and humidity dependency of TGS203 can be compensated to a certain degree in a circuit using a thermistor, as shown in Figure 22.

> Th = Thermistor
> R_{TH} = 8kΩ, B constant = 4200
> R1 = 6.2kΩ
> R2 = 2.24kΩ

Figure 21-2 - Gas detection point

5-4 *FIC-5401*

FIC-5401 is a custom hybrid IC containing the necessary functions for driving the TGS203 and handling output signals for alarm systems. This IC is a useful and convenient item for evaluating the performance of TGS203. For more information about this item and its usage, please refer to the brochure *Product Information - FIC-5401*.
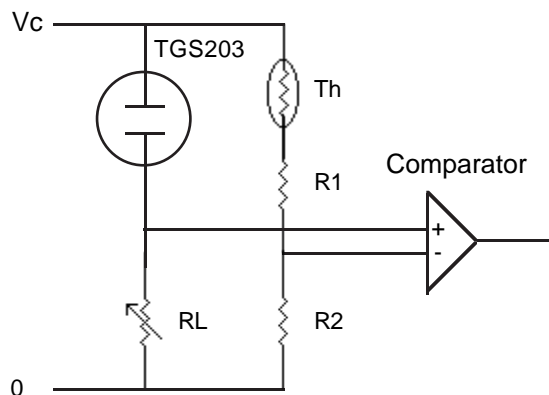

Figure 22 - Temperature compensation circuit